

UWB Wearable Antenna with Full Ground Plane based on PDMS-Embedded Conductive Fabric

Roy B. V. B. Simorangkir, *Student Member, IEEE*, Asimina Kiourti, *Member, IEEE*,
and Karu P. Esselle, *Fellow, IEEE*

Abstract—A new flexible ultra-wideband (UWB) antenna is presented for wearable applications in the 3.7 to 10.3 GHz band, which is highly tolerant to human body loading and physical deformation. The antenna exhibits a footprint of 80 mm × 67 mm and is based on a simple microstrip structure with two modified arc-shaped patches as the main radiator. A full ground plane is maintained on the opposite side of the substrate to suppress antenna loading from the underlying biological tissues and back radiation directed towards the human body. For enhanced flexibility and robustness, the proposed antenna is realized using conductive fabric embedded into polydimethylsiloxane (PDMS) polymer. Promising simulation and experimental results are presented for free-space and *in-vitro* wearable scenarios. To our knowledge, this is the first UWB antenna with a full ground plane that is concurrently highly tolerant to harsh operating conditions, such as those encountered in wearable applications.

Index Terms—Conductive fabric, flexible antenna, fidelity factor, full ground plane, microstrip antenna, polydimethylsiloxane, ultra-wideband, wearable antenna.

I. INTRODUCTION

ULTRA-WIDEBAND (UWB) technology is recently emerging as an attractive solution for several short-range wireless applications, including wireless body-centric networks. Indeed, UWB communications exhibit major advantages as compared to conventional (narrow-band) technologies, including low-power implementations, high-data-rate transmission capabilities, and robustness against multipath [1]. Along these lines, several research efforts have focused on developing flexible and planar UWB antennas for wearable applications [2]–[9]. Flexible materials used for the aforementioned purpose include textiles, liquid metal, paper, copper foil, conductive threads, and polymers.

A common characteristic of most of the previously reported flexible planar UWB antennas is the lack of a full ground plane on the back of the radiator. Instead, partial/modified ground planes or coplanar waveguide topologies are generally preferred as they allow for easy bandwidth enhancement. However, such designs are highly undesirable for wearable applications mainly for two reasons. Firstly, the lack of a full ground plane implies that the high-permittivity and lossy biological tissues will significantly load the antenna, affecting, in turn, its performance. Secondly, those antenna designs are associated with back radiation (i.e., radiation in their lower hemisphere), which, in turn, unavoidably increases the Specific

Absorption Rate (SAR) inside the human body. To mitigate the aforementioned problems, UWB antenna designs equipped with a full ground plane have recently been reported [7], [8]. Although flexible, these prototypes were textile-based, and thus highly sensitive to wetness, heat, and extreme deformations. Consequently, they are unsuitable for harsh operating conditions, such as those encountered in wearable applications.

In this letter, we present a new planar UWB antenna design with suppressed backside radiation, suitable for wearable applications in the 3.7 to 10.3 GHz band. Notably, the antenna is fabricated via polydimethylsiloxane (PDMS)-embedded conductive-fabric technology, which enables conformality, flexibility, easy realization, robustness, water resistance, thermal and chemical stability as demonstrated previously in [10], [11]. Thus, to our knowledge, this is the first-ever flexible and physically robust body-worn UWB antenna with a full ground plane.

The rest of the paper is organized as follows. Section II presents the UWB antenna design. Section III discusses the simulated vs. *in-vitro* antenna performance. The paper concludes in Section IV.

II. UWB ANTENNA TOPOLOGY AND PROTOTYPE

As seen in Fig. 1, the proposed antenna design is based on a simple microstrip patch technology. Two modified arc-shaped patches operating as the main radiator are placed on top of a PDMS substrate, having a relatively constant permittivity of 2.7 and an increasing loss tangent from 0.02 to 0.07 in the FCC UWB bandwidth of 3.1 to 10.6 GHz. On the opposite side of the substrate, a full ground plane is preserved. The entire structure is further encapsulated into PDMS (i.e., PDMS layers are added on top of the radiator and ground plane, respectively).

To realize the conductive antenna parts, two different woven conductive fabrics were employed. Specifically, a nickel-copper-silver coated nylon ripstop from Marktek Inc., having a thickness of 0.13 mm, was used as the patch layer due to its high conductivity. Concurrently, a nickel-copper coated ripstop from Less EMF Inc., having a thickness of 0.08 mm, was used as the ground layer. The latter choice was attributed to its higher porosity than the first fabric which is, in turn, beneficial for the PDMS-fabric adherence over the entire ground plane area [11]. In simulations, both fabrics were modeled with their correspondent thicknesses and were set to effective conductivity values of 1.02×10^5 S/m and 5.4×10^4 S/m, respectively, which were obtained via a transmission line method [11]. It is worth mentioning that these values take into account the

R. B. V. B. Simorangkir and K. P. Esselle are with the School of Engineering, Macquarie University, Sydney, NSW 2109, Australia (e-mail: roy.basten@hdr.mq.edu.au).

A. Kiourti is with the Department of Electrical and Computer Engineering, Ohio State University, Columbus, OH 43212 USA (email: kiourti.1@osu.edu).

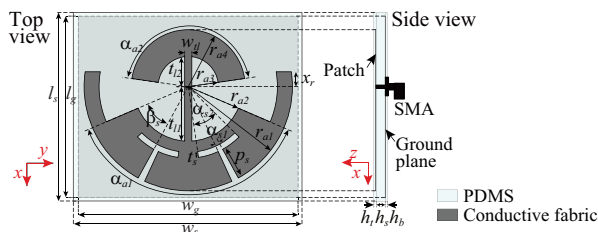


Fig. 1. Detailed geometry of the proposed UWB antenna ($\alpha_{a1} = 134^\circ$, $\alpha_{a2} = 164^\circ$, $r_{a1} = 35.1$, $r_{a2} = 18.4$, $r_{a3} = 10.2$, $r_{a4} = 19.2$, $t_{l1} = 18.3$, $t_{l2} = 10.2$, $w_{tl} = 2.4$, $\alpha_{s1} = 4^\circ$, $\alpha_{s2} = 38^\circ$, $\beta_s = 38^\circ$, $p_s = 11$, $t_s = 2$, $x_r = 5$, $w_g = 74$, $l_g = 61$, $w_s = 80$, $l_s = 67$, $h_t = 0.2$, $h_s = 3$, $h_b = 0.2$). Apart from the angles, all dimensions are in millimeters.

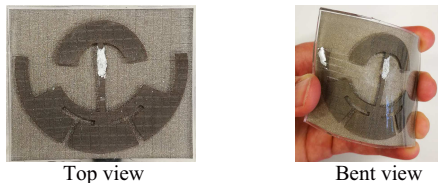


Fig. 2. Photographs of the fabricated UWB antenna.

additional loss likely contributed by the PDMS penetrating into the fabric pores.

As is well known, a conventional thin patch antenna with a full ground plane is inherently narrowband. Thus, to achieve an ultra-wide bandwidth, several bandwidth enhancement techniques, including the use of multiple resonators and slots [12], were applied. Specifically, as seen in Fig. 1, two arc-shaped patches, operating in the higher and lower bands of the desired FCC UWB range, were employed. Each patch was fed by two small transmission lines connected to a coaxial probe on the opposite side of the substrate. To further improve the matching at lower frequencies, two identical T-shaped slots having a length of approximately less than a quarter of the effective wavelength at the lowest target operation frequency (3.1 GHz) were added. An optimization process was further pursued in CST Microwave Studio 2016. The final antenna dimensions are given in the caption of Fig. 1.

Antenna prototyping was performed through the bottom-top multilayer fabrication process described in [10], [11]. To ensure fabrication accuracy, three rectangular ring-shaped molds were used, whose thickness and dimensions matched those of the optimized antenna design. Laser cutting was used for patterning of the radiating patch. For ease of measurements (particularly in the case of *in-vitro* testing), a small 90° bent SMA connector was utilized at the antenna feeding point. Fig. 2 shows the fabricated UWB antenna prototype.

III. UWB ANTENNA PERFORMANCE

Antenna performance was studied in free-space and near-human-body environments. The latter was performed via a flat canonical phantom and an anatomical human head/torso/arm phantom, as shown in Fig. 3. The tissue emulating material was selected so as to accurately mimic the electrical properties of human muscle in a very wide bandwidth (see Fig. 4). The details of the phantom preparation have been described in [10]. The gap between the antenna and the phantom was maintained to 5 mm by means of a small foam block.

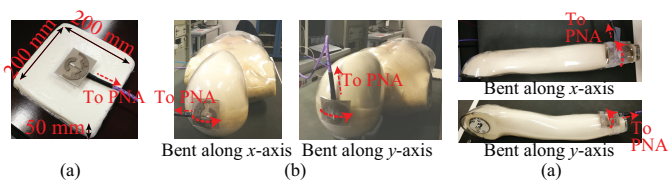


Fig. 3. On-phantom VSWR measurement setups. (a) The antenna placed on top of the flat phantom. The antenna wrapped (b) on the head and (c) on the wrist of the anatomical phantom.

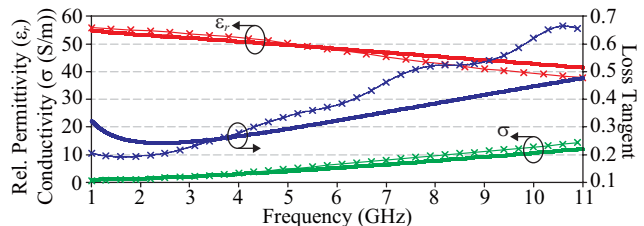


Fig. 4. Measured (solid lines with cross markers) electrical properties of the phantoms compared to the reference database (solid lines) [13].

A. Voltage Standing Wave Ratio (VSWR)

The measured free-space and *in-vitro* (flat phantom) VSWR results are compared with those of simulations in Fig. 5(a). As seen in the simulated results, good matching performance is achieved with a VSWR of below 2 in the frequency range of 3.7 to 10.3 GHz. Remarkably, the VSWR performance is almost identical in free space and when the antenna is placed upon the flat phantom, which signifies that the presence of the full ground plane isolates the antenna from the lossy tissue. As such, good impedance matching can be maintained by the antenna when placed upon the human body. Slight discrepancies are observed in the measured results, which are most likely due to fabrication errors (SMA connector positioning, burnt fabric edges following the laser cutting, etc.).

The effect of antenna deformation upon the VSWR was also investigated. To do so, the antenna prototype was bent around the head and wrist of the anatomical phantom, which have approximate bending radii of 110 and 28 mm, respectively. As shown in Figs. 3(b) and (c), for each position the antenna was bent across both the x -axis and the y -axis. The VSWR performance for the bent antenna setups as compared to the unbent antenna placed upon the flat phantom is shown in Fig. 5(b). As seen, a very stable VSWR is maintained, verifying the robustness of the proposed antenna against physical deformation. Even more importantly, the antenna returned to its original shape after bending, and the conductive fabrics remained intact inside the PDMS encapsulation. The latter is attributed to the PDMS-PDMS bonding formed through the pores of the fabric [11].

B. Far-Field Characteristics

Measured vs. simulated far-field patterns for the antenna are shown in Fig. 6. Two scenarios were considered, viz. antenna in free space (Fig. 6(a)), and antenna placed upon the flat phantom (Fig. 6(b)). In general, a good agreement is achieved between measured and simulated results. As expected, due to the full ground plane, the antenna radiates mainly towards

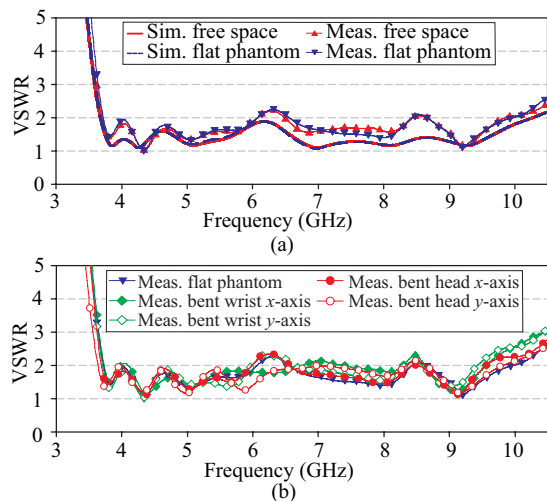


Fig. 5. (a) Simulated and measured VSWR of the unbent antenna in free space and when placed on the flat phantom. (b) Measured VSWR of the antenna when bent on the head and wrist of the anatomical phantom.

its boresight direction. In turn, this minimizes antenna-body coupling and energy dissipation inside the body.

Notably, this mode of directional radiation is maintained even at higher frequencies. When the antenna is placed upon the flat phantom, the patterns are relatively similar to those in free space. Expectedly, even lower back radiation is observed as attributed to the reflection from the phantom. The measured peak gains and efficiencies of the antenna are given in Fig. 7, which are again in good agreement with the corresponding simulated results. From the measurements, the total radiation efficiencies of the antenna are slightly reduced when mounted on the phantom, but thanks to the full ground plane, the difference is less than 5.7% as compared to the free-space scenario. It is also worth noting that the peak gains, particularly at higher frequencies (i.e., above 6.2 GHz), increase when the antenna is in close proximity to the phantom. This is attributed to reflections from the phantom [7], [14].

C. SAR Performance

The impact of the antenna to the underlying human body tissues is investigated by calculating the corresponding SAR distributions in CST Microwave Studio 2016. In this case, the antenna was placed 5 mm above a 200 mm × 200 mm × 50 mm human muscle phantom exhibiting electrical properties same to those obtained from measurements. The SAR values were calculated based on the IEEE C95.1-2005 standard averaged over 10 g of tissue [15], assuming an input power of 0.5 W. Thanks to the isolation provided by the ground plane, the peak SAR results at 5, 7, and 9 GHz were found to be equal to 0.147, 0.174, and 0.09 W/kg, respectively, which conform to the SAR requirement of lower than 2 W/kg [15]. These results further highlight the superiority of the proposed antenna for on-body applications.

D. Time-Domain Performance

The capability of the proposed UWB antenna for a pulse-based transmission was evaluated through a system fidelity analysis in both free-space and on-body environments. To

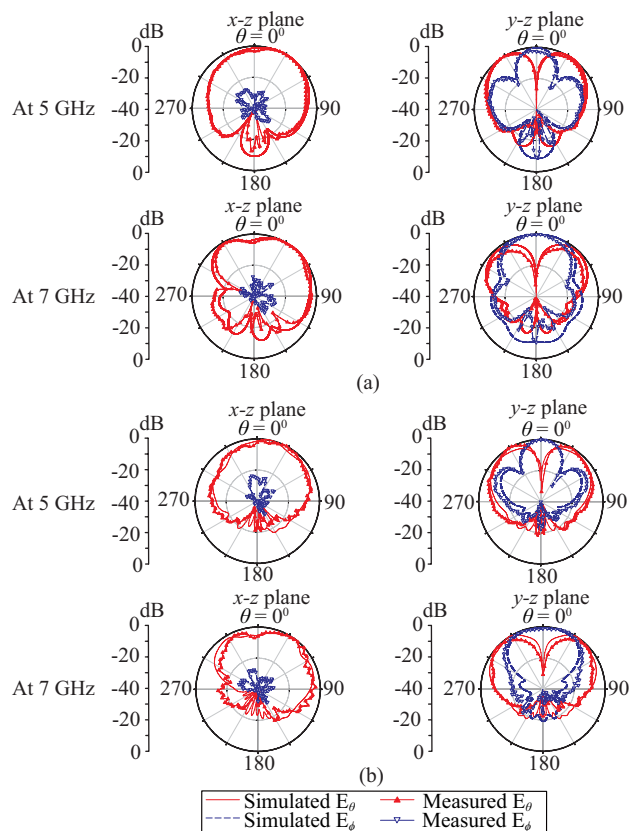


Fig. 6. Normalized radiation patterns of the antenna at 5 and 7 GHz. (a) In free space. (b) On the flat phantom.

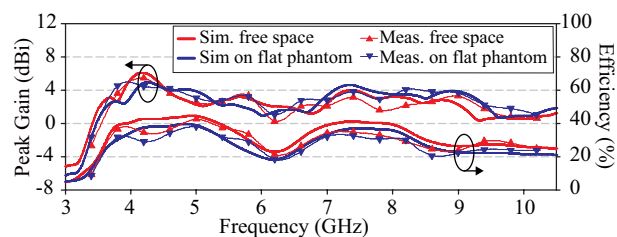


Fig. 7. Simulated and measured peak gains and total efficiencies of the antenna when in free space and on the flat phantom.

do so, two identical UWB antennas were aligned in CST Microwave Studio 2016 across 1 m distance, and the simulated transmission coefficient ($|S_{21}|$) was obtained. For the on-body case, we employed the same human-muscle phantom used in the SAR analysis, yet with a smaller size (110 mm × 110 mm × 50 mm) for reduced computational cost. Again, each antenna was placed at 5 mm distance away from the phantom.

Three sine-modulated Gaussian pulses shown in Fig. 8(a) were used as the transmitted pulses, and were different in terms of center frequency and bandwidth (see Fig. 8(b)). To quantify the antennas ability to preserve the pulse shape, the system fidelity factor (FF) was calculated for both the free-space and on-phantom cases [16]. In free space, the calculated SFF results for pulse I, II, and III were 0.88, 0.77, and 0.72, respectively, whereas on the flat phantom, they were 0.88, 0.79, and 0.68, respectively. In general, it can be noticed

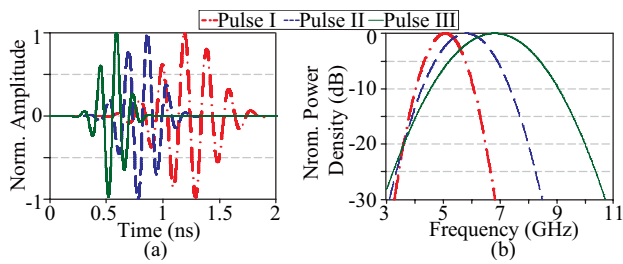


Fig. 8. Different excitation pulses used in the system fidelity analysis. (a) Time-domain waveforms. (b) Power spectral density.

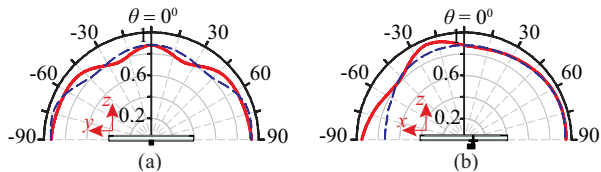


Fig. 9. System fidelity patterns of the proposed UWB antenna in free space (solid lines) and on the flat phantom (dashed lines) obtained from simulations. (a) Horizontal plane. (b) Vertical plane.

that the human body has a small effect on the fidelity of the received pulses. However, the SFF does decrease as the bandwidth of the pulse increases, which might be due to the existence of more spectra of the pulse falling into the lower radiation region of the antenna [17], i.e. 6.2 GHz and above 8.5 GHz. Nevertheless, the values are still higher than the commonly accepted SFF for UWB signal transmission (SFF > 0.5) [16].

The system fidelity patterns of the antenna when pulse I was used as the excitation signal were also obtained. This was performed by rotating the position of the receiver antenna every 15° in both horizontal (y - z) and vertical (x - z) planes, while maintaining the transmitter antenna stationary. Only the patterns for the upper hemisphere of the antenna were observed considering the radiation mechanism of the antenna. The results are given in Figs. 9(a) and (b) for the free-space and on-phantom cases. On the flat phantom, the average SFF values were 0.88 and 0.86 in the horizontal and vertical planes, respectively. These are very close to the free-space case in the horizontal plane (0.88) and vertical plane (0.91).

IV. CONCLUSION

A new flexible planar UWB antenna with a full ground plane has been presented. As opposed to previously reported flexible UWB antennas, the proposed UWB design: a) maintains a full ground plane which delivers the necessary isolation between the antenna and the human body when worn, and b) exhibits extreme physical robustness attributed to the employed PDMS-embedded conductive fabric fabrication technology. On-body measurements upon a phantom show that the antenna achieves a bandwidth of more than 6 GHz (from 3.68 to 10.1 GHz) with VSWR less than 2.2, an average peak gain of 4.53 dBi, and an average total efficiency of 27%, which are quite close to the performance in free space. For an input power of 0.5 W, the SAR levels in the underlying tissues were found to be less than 2 W/kg, implying conformance with international safety guidelines. Time-domain performance investigations

also demonstrated that the proposed antenna is suitable for UWB pulse transmission. In future work, effort will be directed towards reducing the loss of materials and improving the antenna efficiency, particularly at high frequencies. This can be achieved through repeated conductive coating of the fabric and mixing PDMS with other materials.

ACKNOWLEDGMENT

The authors would like to thank Dr. Yang Yang from the University of Technology Sydney for his support during the far-field measurements of the prototype.

REFERENCES

- [1] J. Foerster, E. Green, S. Somayazulu, D. Leeper, I. A. Labs, I. A. Labs, I. Corp, and I. Corp, "Ultra-wideband technology for short-or medium-range wireless communications," *Intel Tech. Journal*, vol. 2, p. 2001.
- [2] M. Klemm and G. Troester, "Textile UWB antennas for wireless body area networks," *IEEE Trans. Antennas Propag.*, vol. 54, no. 11, pp. 3192–3197, Nov 2006.
- [3] S. Cheng, Z. Wu, P. Hallbjorn, K. Hjort, and A. Rydberg, "Foldable and stretchable liquid metal planar inverted cone antenna," *IEEE Trans. Antennas Propag.*, vol. 57, no. 12, pp. 3765–3771, Dec 2009.
- [4] G. Shaker, S. Safavi-Naeini, N. Sangary, and M. M. Tentzeris, "Inkjet printing of ultrawideband (UWB) antennas on paper-based substrates," *IEEE Antennas Wireless Propag. Lett.*, vol. 10, pp. 111–114, 2011.
- [5] Q. H. Abbasi, M. U. Rehman, X. Yang, A. Alomainy, K. Qaraq, and E. Serpedin, "Ultrawideband band-notched flexible antenna for wearable applications," *IEEE Antennas Wireless Propag. Lett.*, vol. 12, pp. 1606–1609, 2013.
- [6] T. I. Yuk, Y. Sun, and S. W. Cheung, "Design of a textile ultra-wideband antenna with stable performance for body-centric wireless communications," *IET Microw., Ant. and Propag.*, vol. 8, no. 15, pp. 1363–1375, dec 2014.
- [7] P. B. Samal, P. J. Soh, and G. A. E. Vandenbosch, "UWB all-textile antenna with full ground plane for off-body WBAN communications," *IEEE Trans. Antennas Propag.*, vol. 62, no. 1, pp. 102–108, Jan 2014.
- [8] L. A. Y. Poffelie, P. J. Soh, S. Yan, and G. A. E. Vandenbosch, "A high-fidelity all-textile UWB antenna with low back radiation for off-body WBAN applications," *IEEE Trans. Antennas Propag.*, vol. 64, no. 2, pp. 757–760, Feb 2016.
- [9] A. da Conceicao Andrade, I. P. Fonseca, S. F. Jilani, and A. Alomainy, "Reconfigurable textile-based ultra-wideband antenna for wearable applications," in *Proc. 10th Eur. Conf. on Ant. and Propag. (EuCAP)*, April 2016, pp. 1–4.
- [10] R. B. V. B. Simorangkir, Y. Yang, K. P. Esselle, and B. A. Zeb, "A method to realize robust flexible electronically tunable antennas using polymer-embedded conductive fabric," *IEEE Trans. Antennas Propag.*, vol. 66, no. 1, pp. 50–58, Jan 2018.
- [11] R. B. V. B. Simorangkir, Y. Yang, and K. P. Esselle, "Robust implementation of flexible wearable antennas with PDMS-embedded conductive fabric," in *Proc. 12th Eur. Conf. on Ant. and Propag. (EuCAP)*, April 2018 (To appear).
- [12] K. L. Wong, "Broadband microstrip antennas," in *Compact and Broadband Microstrip Antenna*. New York: John Wiley & Sons, Inc., 2002, ch. 7, pp. 232–278.
- [13] D. Andreuccetti, R. Fossi, and C. Petrucci, "An internet resource for the calculation of the dielectric properties of body tissues in the frequency range 10 Hz–100 GHz," IFAC-CNR, Florence, Italy, 1997. [Online]. Available: <http://niremf.ifac.cnr.it/tissprop/>
- [14] N. Chahat, M. Zhadobov, R. Sauleau, and K. Ito, "A compact UWB antenna for on-body applications," *IEEE Trans. Antennas Propag.*, vol. 59, no. 4, pp. 1123–1131, April 2011.
- [15] "IEEE Standard for Safety Levels with Respect to Human Exposure to Radio Frequency Electromagnetic Fields, 3 kHz to 300 GHz," *IEEE Std C95.1-2005 (Revision of IEEE Std C95.1-1991)*, pp. 1–238, April 2006.
- [16] G. Quintero, J. F. Zurcher, and A. K. Skriverivik, "System fidelity factor: a new method for comparing UWB antennas," *IEEE Trans. Antennas Propag.*, vol. 59, no. 7, pp. 2502–2512, July 2011.
- [17] M. Koohestani, N. Pires, A. K. Skriverivik, and A. A. Moreira, "Performance study of a UWB antenna in proximity to a human arm," *IEEE Antennas Wireless Propag. Lett.*, vol. 12, pp. 555–558, 2013.